Confirmation of the colonization path of Hymenoscyphus fraxineus from leaves to shoots in Fraxinus excelsior

Astrid Koehl

Année universitaire : 2017-2018 Master Biologie, Agrosciences Parcours Amélioration, Production, Valorisation du végétal Option Physiologie Moléculaire et Adaptations aux Stress	**Rapport de stage** ☐ d'Ingénieur de l'Institut Supérieur des Sciences agronomiques, agroalimentaires, horticoles et du paysage ☑ de Master de l'Institut Supérieur des Sciences agronomiques, agroalimentaires, horticoles et du paysage ☐ d'un autre établissement (étudiant arrivé en M2)

Confirmation of the colonization path of *Hymenoscyphus fraxineus* from leaves to shoots in *Fraxinus excelsior*

Par : Astrid KOEHL

Soutenu à Rennes le 28 juin 2018

Devant le jury composé de :

Président : Antoine GRAVOT

Maître de stage : Thomas KIRISITS

Tuteur : Antoine GRAVOT

Rapporteur : Francisco CABELLO HURTADO

Examinateur : Régine DELOURME

Fiche de confidentialité et de diffusion du mémoire

Confidentialité

☑ Non ☐ Oui   si oui :   ☐ 1 an   ☐ 5 ans   ☐ 10 ans

Pendant toute la durée de confidentialité, aucune diffusion du mémoire n'est possible [1].

Date et signature du maître de stage [2] :

A la fin de la période de confidentialité, sa diffusion est soumise aux règles ci-dessous (droits d'auteur et autorisation de diffusion par l'enseignant à renseigner).

Droits d'auteur

L'auteur[3] **Koehl Astrid**
autorise la diffusion de son travail (immédiatement ou à la fin de la période de confidentialité)

☑ Oui   ☐ Non

Si oui, il autorise

☐ la diffusion papier du mémoire uniquement(4)

☐ la diffusion papier du mémoire et la diffusion électronique du résumé

☑ la diffusion papier et électronique du mémoire (joindre dans ce cas la fiche de conformité du mémoire numérique et le contrat de diffusion)

(Facultatif) ☑ accepte de placer son mémoire sous licence Creative commons CC-By-Nc-Nd (voir Guide du mémoire Chap 1.4 page 6)

Date et signature de l'auteur : 13/07/2018

Autorisation de diffusion par le responsable de spécialisation ou son représentant

L'enseignant juge le mémoire de qualité suffisante pour être diffusé (immédiatement ou à la fin de la période de confidentialité)

☐ Oui   ☐ Non

Si non, seul le titre du mémoire apparaîtra dans les bases de données.
Si oui, il autorise

☐ la diffusion papier du mémoire uniquement(4)

☐ la diffusion papier du mémoire et la diffusion électronique du résumé

☐ la diffusion papier et électronique du mémoire

Date et signature de l'enseignant :

(1) L'administration, les enseignants et les différents services de documentation d'AGROCAMPUS OUEST s'engagent à respecter cette confidentialité.
(2) Signature et cachet de l'organisme
(3) Auteur = étudiant qui réalise son mémoire de fin d'études
(4) La référence bibliographique (= Nom de l'auteur, titre du mémoire, année de soutenance, diplôme, spécialité et spécialisation/Option)) sera signalée dans les bases de données documentaires sans le résumé

Dépôt numérique de mémoire
ATTESTATION DE CONFORMITE DE LA VERSION NUMERIQUE

Je, soussigné(e),

Nom : Koehl

Prénom : Astrid

Ci-après désigné « l'Auteur »

Atteste que la version numérique de mon mémoire de fin d'études dans sa version définitive (incluant les corrections demandées par le jury de soutenance),
Intitule

Confirmation of the colonization path of Hymenoscyphus fraxineus from leaves to shoots in Fraxinus excelsior

correspond à la version imprimée du document, déposé à la bibliothèque générale d'AGROCAMPUS OUEST (CFR de référence)

A Rennes le 13/07/2018

Signature

Dépôt numérique de mémoire
CONTRAT DE DIFFUSION NUMERIQUE DE MEMOIRE

Entre

AGROCAMPUS OUEST, Institut supérieur des sciences agronomiques, agroalimentaires, horticoles et du paysage dont le siège est basé 65 rue de Saint-Brieuc, 35042 RENNES, représenté par son Directeur Général, Grégoire THOMAS

et

L'auteure du mémoire :
Nom : Koehl
Prénom : Astrid
Adresse personnelle : 16, rue de Plaisance 35310 MORDELLES
Intitulé du mémoire : **Confirmation of the colonization path of Hymenoscyphus fraxineus from leaves to shoots in Fraxinus excelsior**

Ci-après désigné auteur,

Article 1
Le présent contrat ne concerne que les mémoires de fin d'études des cursus de formation d'AGROCAMPUS OUEST, déposés suite à la soutenance dans leur version validée par le jury. La diffusion de ces mémoires est conditionnée au visa du responsable de spécialisation/ option, garantissant la prise en compte de l'avis du jury.

Article 2
L'auteur autorise AGROCAMPUS OUEST à diffuser le mémoire sur le site Internet de l'établissement ou sur les plateformes choisies par AGROCAMPUS OUEST en conformité avec la fiche de diffusion correspondante. Le présent contrat a pour objet de permettre à AGROCAMPUS OUEST de diffuser le mémoire dans le respect des droits de propriété intellectuelle de son auteur.
Le présent contrat n'implique pas l'obligation pour AGROCAMPUS OUEST de faire usage de l'autorisation qui lui est donnée. La diffusion effective, tout comme son éventuelle suppression, n'implique en aucun cas une appréciation au bénéfice de l'auteur ou des tiers et n'est pas source de responsabilité à l'égard des tiers.

Article 3
L'auteur demeure responsable du contenu de son œuvre. L'auteur garantit à AGROCAMPUS OUEST qu'il détient tous les droits nécessaires à la diffusion de son œuvre, en particulier les autorisations écrites des titulaires des droits sur les œuvres reproduites, partiellement ou intégralement. En cas de non respect de cette clause, AGROCAMPUS OUEST se réserve le droit de refuser, suspendre ou arrêter la diffusion des parties du mémoire intégrant des documents ou parties de documents pour lesquels les droits de reproduction et de représentation n'auraient pas été acquis.
AGROCAMPUS OUEST ne pourra être tenu responsable de représentations illégales de documents, pour lesquels l'auteur n'aurait pas signalé qu'il n'en avait pas acquis les droits.

Article 4
L'auteur pourra à tout moment retirer l'autorisation de diffusion qu'il accorde par le présent contrat. Pour cela, il devra en aviser formellement AGROCAMPUS OUEST par lettre recommandée avec accusé de réception. AGROCAMPUS OUEST aura alors l'obligation de retirer l'œuvre lors de la plus prochaine actualisation du site de l'établissement et du portail documentaire.

Article 5

L'auteur autorise AGROCAMPUS OUEST à procéder, le cas échéant, au reformatage de son mémoire en vue de l'archivage, de la diffusion ou de la communication dans le respect des autorisations de diffusion définies par lui précédemment.

Article 6

Les autorisations de diffusion données à AGROCAMPUS OUEST n'ont aucun caractère exclusif et l'auteur conserve toutes les autres possibilités de diffusion de son mémoire.

Article 7

L'auteur autorise, à titre gracieux, la cession des droits de diffusion, concernant le mémoire qui lui appartient. Cette autorisation, dans la durée maximale définie par le droit patrimonial, est strictement réservée à la diffusion du mémoire à des fins pédagogiques et de recherche.

Fait à Rennes le 13/07/2018

Pour AGROCAMPUS OUEST,
L'auteur,
Pour Le Directeur Général
Et par délégation,

Acknowledgments

Table of Contents

1. Introduction

1.1. History of ash dieback

European ash dieback (ADB) is a highly destructive disease killing ash trees (*Fraxinus excelsior*) in large parts of Europe. After its first observation in Poland and Lithuania in the early to mid-1990s, ADB has spread across Europe over the past 25 years from east to west (Kowalski, 2006; Timmermann *et al.*, 2011; Kjær *et al.*, 2012). The disease has now been reported in most of Europe and was even detected in the British Islands and in Ireland in 2012.

The pathogenic agent responsible for the disease was identified in 2006 and named *Chalara fraxinea* (Kowalski, 2006), based on the morphology of its asexual structures. However, with the aid of molecular methods, the fungus was later assigned to the genus *Hymenoscyphus*. For a short while, it was confused with its cryptic sister species *Hymenoscyphus albidus* but was then recognized as a separate taxon (now known under the name *Hymenoscyphus fraxineus*, see below). Actually, *H. albidus* is an avirulent species closely related to the pathogen but there are well established species barriers (Wey *et al.*, 2016). In fact, co-occurrence has been reported but no hybridization had been found in nature between the two species so far (Husson *et al.*, 2011; Queloz *et al.*, 2011). *H. albidus* is an indigenous European foliage colonizer which decomposes *Fraxinus excelsior* leaves and is non-pathogenic on *F. excelsior* (Baral & Bemmann, 2014; Kowalski *et al.*, 2015). It has been hypothesized that the endemic *H. albidus* could be replaced by the alien species causing ADB which could lead to extinction of the former species through competitive exclusion (McKinney *et al.*, 2012). Molecular differentiation led to the recognition that the two *Hymenoscyphus* species were indeed distinct, and hence a new name was given to the pathogenic species: *Hymenoscyphus pseudoalbidus (*Queloz *et al.*, 2011). However, the scientific name of the pathogen has been changed recently and is now *Hymenoscyphus fraxineus* (Baral *et al.*, 2014).

In its natural habitat, *H. fraxineus* is a nearly harmless leaf endophyte found in Eastern Asia (Japan, Korea, northeast of China, Russian Far East) on *Fraxinus mandshurica*, the Manchurian ash, and *F. chinensis* spp. *Rhynchophylla*, the Korean ash (Cleary *et al.*, 2016; Zhao *et al.*, 2012; Gross *et al.* 2014). However, Drenkhan *et al.* (2017) reported the association of *H. fraxineus* with symptoms on leaves and possibly also on twigs of both Manchurian and Korean ash in Russian Far East. This indicates that the fungus was an overlooked weak pathogen in its natural environment prior to having received attention due to the ash dieback epidemic in Europe. A recent study suggests that the European population was founded by two individuals from a large diverse population originating from East Asia (McMullan *et al.*, 2018).

1.2. Impact on *Fraxinus excelsior*

Common ash (*F. excelsior*) is an important forest tree in Europe. Its timber is mainly used for floors and furniture. However, its ecological value is even more substantial. For example, in the British Islands, almost a thousand species are associated with *F. excelsior* and forty are obligate associates. Furthermore, if a shift of woodland composition happens towards other tree species as a result of ADB, it would change nutrient cycling, carbon storage, and soil formation, which would drive shifts in the soil community (Mitchell *et al.*, 2014).

In Sweden, about 60 species associated with common ash (and *F. excelsior* itself) have been put on the Sweden red-list of threatened species because of damages caused by *H. fraxineus*. Finally, the disease also has a cultural impact. Indeed, trees are not only affected in forests, but also in parks and gardens.

This devastating pathogen is capable of colonizing every part of *F. excelsior*: leaves, shoots, main stems and even roots (Kirisits *et al.*, 2009; Schumacher *et al.*, 2010; Husson *et al.* 2012; Gross *et al.*, 2014; Schwanda & Kirisits, 2016). *H. fraxineus* is an aggressive invasive pathogen which is particularly damaging on young ash trees, often killing them within one growing season after infection. Older trees can survive initial infections, but become chronically diseased and tend to succumb after several seasons due to secondary diseases such as root and butt rot caused by *Armillaria* species (Skovsgaard *et al.*, 2010; Chandelier *et al.*, 2016). On a European scale, current levels of *H. fraxineus* may infect and kill 95% of all European ash trees (McMullan *et al.*, 2018).

Many studies have evaluated in detail the damage levels caused by *H. fraxineus* on *F. excelsior* in different European countries. For example, in a young ash plantation in Germany, 73% of the saplings were dead five years after planting (Langer *et al.*, 2015). In Norway, a mortality rate of 57% was observed on monitoring plots in ash forests in 2016 (Timmermann *et al.*, 2017). Furthermore, a relationship between the severity of infection and the age of the trees was detected. In the natural forests monitoring in Norway, 80% of young trees were dead in 2016, whereas for older trees, the mortality was only around 20% (Timmermann *et al.*, 2017). In France and Belgium, survey found an annual mortality rate of 35% in younger ash stands and only 3% in older stands (Marçais *et al.*, 2017).

1.3. Host-pathogen interactions

It is estimated than less than 5% of ash trees are partially resistant or tolerant to ADB (Kjær *et al.*, 2012; Sollars *et al.*, 2017). Overall comprehension of the metabolic pathways of the interaction between *F. excelsior* and *H. fraxineus* (both on the host side and pathogen side) is still incomplete but new insights start to unravel some parts of this metabolic network.

The level of susceptibility of *F. excelsior* to *H. fraxineus* has been recently associated with the abundance of iridoid glycosides, which are part of a well-known anti-herbivore defense mechanism in the Oleaceae, also capable of enhancing fungal growth (Sollars *et al.*, 2017). Thus, their findings suggest that there might be a trade-off between ADB susceptibility and herbivore susceptibility.

Some of the pathogen effectors have been described (McMullan *et al.*, 2018). They present an NPP1 (necrosis-inducing Phytophthora protein) domain, which is present in fungal proteins that induce hypersensitive-reaction-like cell death when infiltrating plant leaves. Their presence seems to be common among necrotrophic parasites, to which *H. fraxineus* also belongs. Furthermore, *H. fraxineus* has a large number of predicted secreted Cytochrome P450 proteins, which might play a role in pathogenesis (McMullan *et al.*, 2018). Cytochrome P450s' modes of action are usually via the monooxygenase reaction. Potential roles for P450s in *H. fraxineus* include i) destruction of ash aromatic compounds with antifungal properties, ii) penetration of ash tree tissues through degradation of hydrocarbon compounds, the main constituents of the cuticle and iii) secretion of toxins during invasion of ash tree tissues.

Figure 1: Symptoms of ash dieback on *Fraxinus excelsior*. (a) necrotic spots on a leaflet; (b),(c) necrotic lesions on leaflet midribs and adjacent leaf blade tissues; (d) leaf wilting distal to a necrotic lesion on the rachis; (e),(f) necrotic bark lesion on a shoot originating from an infected side leaf and twig; (g) extensive bark necrosis leading to shoot dieback; (h) wood discoloration beneath a necrotic bark lesion on a shoot; (i),(j) tongue-shaped bark lesions at the base of *F. excelsior* trunks; (k) wedge-shaped wood discoloration beneath a root collar lesion.

Also, it has been described that *H. fraxineus* produce secondary metabolites such as viridian, a mycotoxin, and its dihydroderivative viridiol, a phytotoxine (Grad *et al.*, 2009). Viridiol might be involved in the development of ADB, especially with the induction and expansion of necrotic spots.

Even if progress still need to be made in order to understand *H. fraxineus* metabolic pathways and how *F. excelsior* defend itself against the pathogen, the symptoms of ash dieback are well-known and allow fast and accurate detection.

1.4. Symptoms of ash dieback

H. fraxineus causes necrotic lesions on leaves and lesions, cankers and wood discoloration in the bark and on the root collar (figure 1). Initially, small necrotic spots and necrotic lesions appear on leaves (Gross *et al.*, 2014). The latter usually form along leaflet veins, from where they expand into petioles. Leaf infections often result in premature shedding of leaflets and entire leaves. From a small portion of these infections, *H. fraxineus* is supposed to penetrate into shoots, twigs and branches where, after an incubation period, necrotic lesions and perennial cankers form. Necrotic lesions and cankers often lead to girdling of woody parts, resulting in wilting of the foliage and crown dieback. Trees respond to infections by prolific production of epicormic shoots leading to a short- to medium term partial restoration of the crown. Necrosis in shoots is assumed to develop mainly after infection through leaf petioles. First appearance of bark lesions from infections in the same year occurs during late summer, but most lesions emerge during autumn and winter, and they can even become visible as late as in late spring or early summer of the next year (Kirisits *et al.*, 2009, 2012; Gross *et al.*, 2014).

Besides crown damage, serious symptoms of ash dieback are necrotic lesions and wood discolorations on the trunk base and root collar (figure 1). These are caused by *H. fraxineus*, likely by germinating ascospores penetrating the intact bark via lenticels (Husson *et al.*, 2012; Chandelier *et al.*, 2016). Such lesions act as entrance courts for *Armillaria* species and other secondary pathogens which cause root an butt rot, destabilizes trees and predisposes them to fall over (Husson *et al.*, 2012; Chandelier *et al.*, 2016). The attacks also drive mortality of ash trees (Marçais *et al.*, 2017).

Accumulating knowledge on the symptoms of ash dieback and their timing, together with overall knowledge on the biology of *H. fraxineus*, and ascomycetes in general, permitted to develop a hypothetic life cycle for the pathogen and a disease cycle of ash dieback.

1.5. Life cycle of *Hymenoscyphus fraxineus*

Some well-known parts of the life cycle in ascomycetes have not yet been described for *H. fraxineus*. This is why some interactions are supposed, but need to be verified. All the main steps are summarized in figure 2.

By early summer, ascogonia develop on old fallen leaf rachises and are probably fertilized by contact with conidia or by mycelium of germinated conidia, if strains of opposite mating types are present. Sexual reproduction in ascomycetes is governed by the mating type locus *MAT*, harboring different *MAT* genes. In heterothallic fungi, like *H. fraxineus*, the *MAT* genes are separated in a bipolar manner (*MAT1-1* and *MAT1-2*) and only individuals with complementary *MAT* idiomorphs are able to mate (Wy *et al.*, 2016; Gross *et al.*, 2012b).
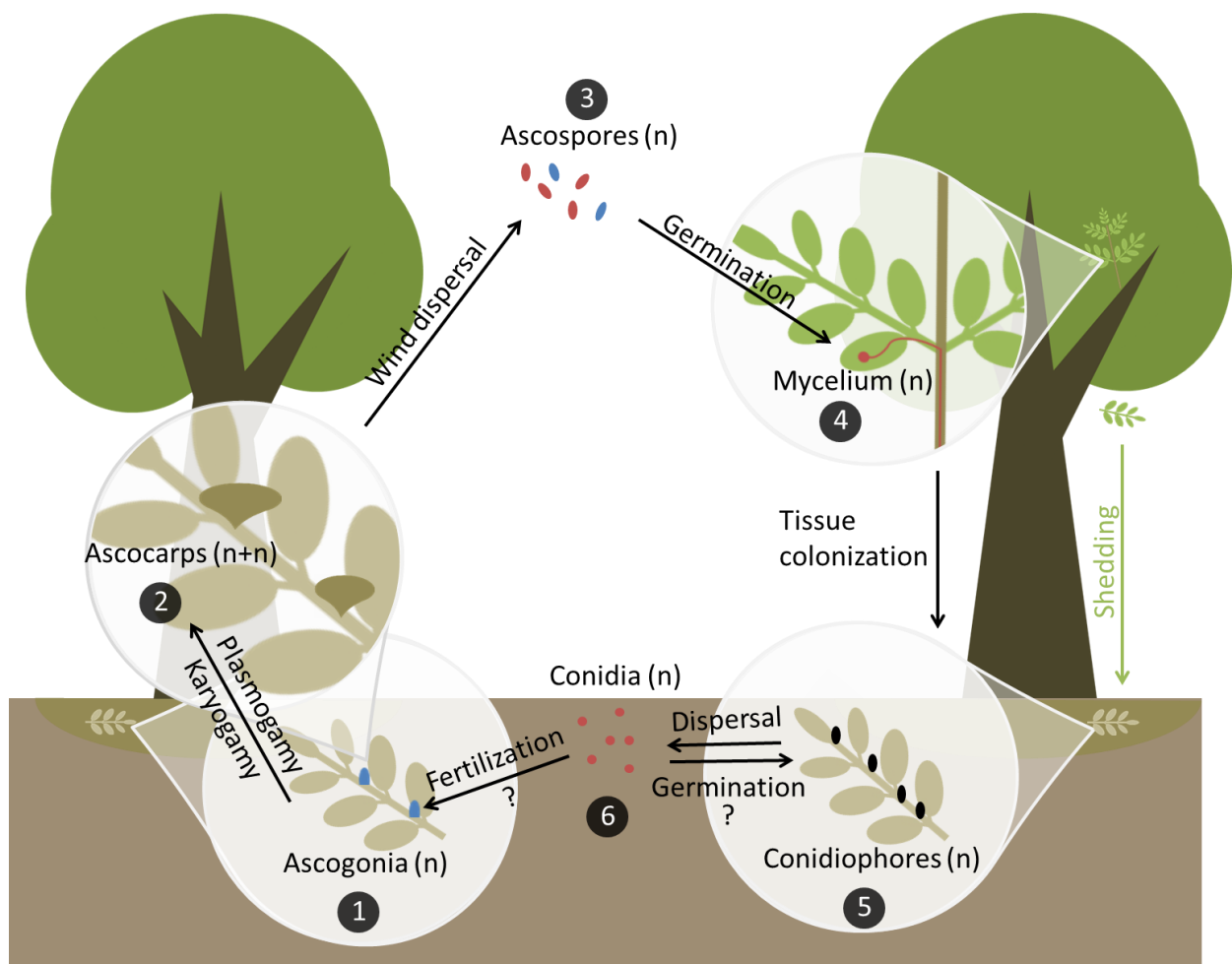
Figure 2: Hypothetical life cycle of *Hymenoscyphus fraxineus*. (1) By early summer, ascogonia develop on old fallen leaf rachises and are probably fertilized by contact with conidia or by the mycelium of germinated conidia, if strains of opposite mating types are present. (2) After plasmogamy, ascocarps form. Karyogamy and then meiosis takes place, resulting in the formation of ascospores. (3) Ascospores are actively released and dispersed by wind. They can land on ash leaves from early summer onwards. (4) With the help of an appressorium, the ascospore penetrates and colonizes susceptible ash leaflet tissues and can then spread to all tree parts. (5) Infected leaves are shed in late summer or early autumn, the fungus overwinters in the leaf litter and develops conidiophores in the same year and during the next season, which produce conidia. (6) Conidia could lead both to sexual and asexual reproduction as they can maybe germinate and encounter ascogonia or germinate and produce other conidiophores. Interrogation marks indicate interactions known in ascomycetes' life cycle which have not described for *H. fraxineus*. The colors red and blue correspond to the two different mating types (*MAT1-1* or *MAT1-2*).

After plasmogamy, ascocarps are formed. Karyogamy and then meiosis takes place, resulting in the formation of ascospores which are actively released and dispersed by wind. They can land on ash leaves in early summer. *H. fraxineus* spreads by producing airborne ascospores on a massive scale, indicating that ascospores play a significant (and probably exclusive) role in infection and long-distance dispersal and that propagule pressure might be a major strategy for colonization success (Gross *et al.*, 2012a, 2012b; Drenkhan *et al.*, 2017). Indeed, it has been shown that initiation of ascospore production by *H. fraxineus* after overwintering is followed by pathogen accumulation in asymptomatic leaves (Cross *et al.*, 2016).

When in contact with a compatible host, a susceptible *Fraxinus* species, an ascospore from *H. fraxineus* will develop an appresorium on the leaf surface to penetrate an epidermal cell. If penetration is successful, the pathogen is able to expand in leaf tissues and some infections spread towards the shoot and further into woody parts. Remarkably, *H. fraxineus* is able to colonize all cell types in all parts of common ash trees. This unusual behavior can be explained by the lack of co-evolution between the alien invasive pathogen and its naïve European host. When infected leaves are shed in late summer or early autumn, the fungus overwinters on the leaf petioles and rachises in the leaf litter, and develops conidiophores in the same year and during the next season. On these asexual fruiting structures conidia are produced. They could both facilitate sexual reproduction, by acting as fertilizing spermatia (directly by contact or indirectly by germination and hyphal contact with ascogonia), and lead to asexual reproduction through germination and hyphal proliferation and production of further conidiophores. They could even be infectious (Fones *et al.*, 2016), although most studies agree that the asexual spores of *H. fraxineus* do not germinate, and are thus exclusively spermatia, not playing a role in the infection biology of the pathogen (Kirisits *et al.*, 2009, 2013; Gross *et al.*, 2012b, 2014; Haňáčková *et al.*, 2017). Clearly, more research is needed to unravel the definite role of conidia in the biology of the ash dieback pathogen.

1.6. Objectives

The main objective of this work was to provide new insights on the life cycle of *H. fraxineus* and to the disease cycle of ash dieback, more specifically, on the colonization path of the pathogen from leaves to shoots of *F. excelsior*.

Here, we used 18 microsatellites markers to analyze 84 isolates obtained from petiole and shoot fragments of 42 *F. excelsior* saplings. The specific goals of the work were to i) identify differentially encoded alleles, ii) establish genetic profiles to characterize individuals and iii) thereby confirm the progression of *H. fraxineus* from petioles to adjacent shoots.

In this work, we chose to use microsatellite markers over internal transcribed spacers (ITS), which are largely used in fungal barcoding, because they are not capable of discriminating genotypes at the individual level. A microsatellite is a tract of DNA motifs repeated in tandems. All of the microsatellites used here are intergenic (non-coding) DNA in the nuclear genome (Gross *et al.*, 2012a; Haňáčková *et al.*, 2015). In order to be used as markers, they need to be selectively neutral, not linked among loci, inherited according to Mendel's laws and polymorphic. Their sequence can be altered through replication slippage, which will result in a gain or a loss of an entire repeat motif, or through point mutations (indels), which affect only one single nucleotide.

Table 1: Collection sites, years of sampling and number of leaf petiole-shoot pairs with fresh symptoms of ash dieback (originating from infections in the year of collection) from which fungal isolations were made.

Site	Geographic coordinates	Elevation (m)	Year[1]	N° of samples[2]
Hernals / site 1	48.24839 N, 16.26868 E	332	2016	4 / 4
Hernals / site 2	48.24153 N, 16.27634 E	280	2016	12 / 8
Hernals / site 3	48.24128 N, 16.27559 E	278	2016	2 / 1
Hernals / site 4	48.24082 N, 16.27667 E	276	2016	15 / 12
Hernals / site 5	48.24043 N, 16.27660 E	276	2016	1 / 0
Hernals / site 6	48.24096 N, 16.27857 E	277	2016	3 / 3
Hernals / site 7	48.24134 N, 16.27707 E	281	2016	5 / 5
Hernals / site 8	48.23923 N, 16.27517 E	281	2016	4 / 4
Hernals / site 9	48.23123 N, 16.28754 E	344	2017	2 / 2[3]
Hernals / site 10	48.24127 N, 16.27876 E	281	2017	4 / 2[4]
Hernals / site 11	48.23788 N, 16.27206 E	294	2017	1 / 1
Zagersdorf / site 12	47.75394 N, 16.53356 E	255	2016	1 / 1

[1]Sampling and fungal isolation was done in late August, September and October 2016 as well as in October 2017; [2]Leaf petiole-shoot pairs; the first number refers to the number of pairs from which fungal isolations were made, the second number refers to pairs from which *H. fraxineus* was both isolated in leaf petiole and the adjacent shoot. These latter isolates were examined in detail in this work; [3]From one petiole-shoot pair at site 9 not only one but three shoot isolates obtained from three different positions of a single shoot were included; [4]Three shoot isolates obtained from three different positions of a single shoot at site 10 were additionally included in the microsatellite analysis although *H. fraxineus* was not isolated from the corresponding petiole.

Figure 3: Example of general state of leaves and shoots before sampling on tree n°58 and tree n°52; (a) necrotic lesion is visible on bark and the leaf is dry and ready to fall; (b) no necrotic lesion is visible on bark but the leaf is wilting and the petiole is necrotic.

2. Material and Methods

2.1. Collection sites and ash sampling

The samples for this work were collected in late August, September and October 2016 as well as in October 2017 in the 17th district of Vienna (Hernals), Austria, at 11 different sites (table 1). The maximum distance between two sites was about 2.25km, but many sites were located within short distances (20-100m) to each other. In addition, one leaf petiole-shoot pair was collected in Zagersdorf (Austrian province of Burgenland; table 1). Each site was woodland of broadleaved trees (various species) with natural regeneration of common ash (*F. excelsior*) in the understorey. The sites were non-systematically chosen based on observations of ash saplings showing appropriate symptoms for this study.

At each sampling date, ash seedlings were carefully inspected for necrotic lesions caused by *H. fraxineus* on the leaf petiole close to the leaf node where it was suspected that the pathogen could have already progressed into the adjacent shoot/seedling stem via the petiole-shoot junction. On some shoots, a necrotic lesion on the bark surface adjacent to a symptomatic leaf petiole was already visible. If this was not the case, one or several small incisions were carefully cut into the bark of the shoot, in order to check whether the phloem around a leaf node was necrotic, indicating a fresh infection by the ADB pathogen. Shoots where several overlapping infections were suspected to occur (indicated by extensive bark necrosis) were not considered for sampling. When necrosis of tissues was confirmed both on a leaf petiole and an adjacent shoot, this leaf petiole-shoot pair was sampled, placed individually in an envelope or plastic bag and transported to the laboratory. Samples were refrigerated (at 4 to 6°C) until they were processed for fungal isolation.

In total, 54 leaf petiole-shoot pairs were collected, 46 in 2016 and 8 in 2017 (table 1). The ash saplings from where samples were taken ranged in height from about 20cm to about 2.5m, and the shoot samples had diameters between 1 and 9mm. The condition of the sampled leaf petioles was variable. While some were totally necrotic and dry but still attached to the shoot, others were still alive and partly green but showed distinct necrotic lesions (figure 3).

2.2. Fungal isolation and identification

From 49 leaf petiole-shoot pairs, fungal isolation was made within two days after collection, from two pairs three days after collection and from three pairs 18 or 19 days after collection. Isolations were done under sterile conditions in a laminar flow. Isolation methods were similar to those described by Kirisits (2017). Malt extract agar (MEA; 20 g DiaMalt malt extract [Hefe Schweiz AG, Stettfurt, Switzerland], 16 g Becoagar agar [W. Behrens & Co., Hamburg, Germany], 1000 ml tap water, 100 mg streptomycin sulphate [Calbiochem; Merck KGaA, Darmstadt, Germany], added after autoclaving) poured in 5.2cm diameter plastic Petri dishes was used as medium.

For fungal isolation, leaf petiole and shoot sections, about 5-8cm long, were surface sterilized; leaf petioles for 30sec in 96% ethanol, 1min in 4% NaClO and 30sec in 96% ethanol, and shoot samples for 1min in 96% ethanol, 3min in 4% NaClO and 30sec in 96% ethanol. The surface sterilized plant parts were then dried for a few minutes, in order to let the ethanol evaporate. From a leaf petiole, the epidermis was carefully scraped off with a sterile scalpel, and an approximately 3-5mm wide part at the base of the petiole was cut away with sterile garden scissors.

Table 2: Primers for *MAT* multiplex PCR. F stands for forward and R for reverse primer. The allele size refers to the expected size of the PCR products visible on the gel (Gross *et al.*, 2012b).

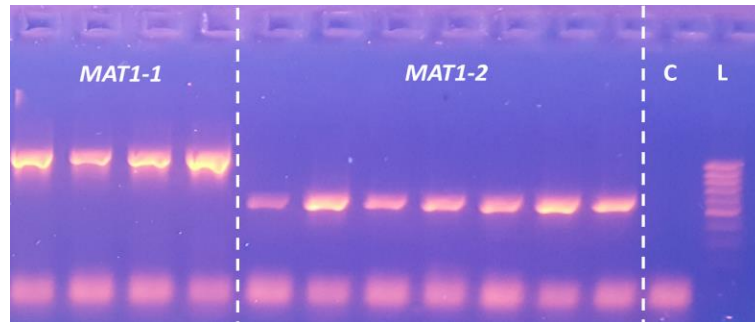| Target	Locus	Primer sequence (5'-3')	Allele size (bp)
MAT1-1 idiomorph	*MAT*	F: TCCTTCGAACCCAAACACCT	1207
		R: GCATATCATCGGCTGCCTTG	
MAT1-2 idiomorph	*MAT*	F: CGCTTTCAGGTATGTCTA	571
		R: TGATACTGGTAGTTCGGATA	

Figure 4: Gel-electrophoresis showing amplified fragments of *Hymenoscyphus fraxineus MAT1-1* and *MAT1-2* idiomorphs. In this example, positive results from several samples are shown. L stands for ladder and C for negative control.

4-6 small fragments were then cut consecutively from the petiole and placed onto a single MEA plate. Similarly, from a shoot section, the outer bark was cut off superficially with a sterile scalpel, and 4-6 small shoot discs (comprising wood and phloem) were cut and put onto one MEA plate. Removal of discs started at or near the proximal edge of the phloem necrosis and adjacent wood discoloration. From two shoots, samples were each taken at three different positions: i) close to the leaf scar where the infection likely originated, ii) at the proximal lesion margin and iii) at a position in between. Petiole fragments and shoot discs removed for fungal isolation were 1-2mm (only occasionally up to 3mm) wide, and samples from a single petiole or shoot were placed well separated from each other onto a single MEA plate, so that well-defined individual fungal colonies could develop. The consecutive order of the pieces along a petiole or shoot was, however, not marked on the isolation plates.

The Petri dishes with the primary isolations were incubated at room temperature and diffuse daylight in the laboratory, and repeatedly inspected for the growth of *H. fraxineus* and other fungi during a two months period. The ADB pathogen was identified based on the morphology of its colony and morphological characteristics of its asexual stage (phialophores, phialids and conidia; Kowalski 2006; Gross *et al.* 2014). Colonies of other fungi were recorded, but they were not identified. *H. fraxineus* isolates were sub-cultured on ash leaf malt extract agar (AMEA; 20g DiaMalt malt extract, 16g Becoagar agar, 50g frozen *F. excelsior* leaflets [which were removed after autoclaving], 1000mL tap water), which greatly enhances the fungus's growth (Kirisits *et al.*, 2013; Gross *et al.*, 2014). Pure cultures and the majority of the primary isolation plates were stored at 4-6°C until further use for this thesis from January 2018 onwards.

2.3. DNA extraction

H. fraxineus isolates were grown on AMEA (prepared with frozen leaflets of *F. mandshurica* seedlings) for three to four weeks. Genomic DNA from *H. fraxineus* isolates was extracted using DNeasy Plant Mini Kit (Qiagen) with minor changes from manufacturer's instructions. Mycelium was scraped and grinded in 70µL of Buffer AP1 with a 4mm steel ball using a Mixer Mill MM 2000 (Retsch). Then, after adding 330µL of Buffer AP1 and 4µL of RNase A (100mg/mL), samples were incubated for 3h at 55°C. Samples were finally eluted in 70µL two times.

2.4. Mating type determination

2.4.1. Multiplex PCR

Each reaction was set up in 10µL volumes containing 4.7µL of PCR water, 1x of S-Buffer (PeqLab), 1mg.mL^{-1} of Bovine Serum Albumin (BSA), 800µM of dNTPs, 0.5µM of each primer (table 2), 0.5U of Taq polymerase (PeqLab) and 1µL of the template DNA (or PCR water for negative control). PCR conditions were 3min at 94°C and continued with 34 cycles at 94°C for 30sec, 55°C for 45sec, 72°C for 45sec then followed by a final extension at 72°C for 5min. PCR amplification was verified on 1.5% agarose gel stained with GelRed Nucleic Acid Gel Stain (Biotum). Gel-electrophoresis was accomplished with 1.7µL of PCR product mixed with 6.2µL of loading buffer. The amplified fragments were visualized on a UV-transilluminator (UVP) after 20min (figure 4). A 100bp-1kb DNA ladder (Biozym) was included in each gel.

Determining mating types is a fast and easy method which was used here to detect some differences in a sample pair (petiole and shoot) at an early stage of the experiment.

Table 3: Primers for microsatellite markers' multiplex PCR. F stands for forward and R for reverse primer. Each locus is given a short code name (L1-L18) corresponding to their order in this table.

Multiplex PCR	Locus		Primer sequence (5'-3')	Dye	Final primer concentration in PCR [µM]	Reference
A	L1	*mHp_067022*	F: CGCACGAAAACGAAAGTCTA	FAM	0,2	Gross *et al.*, 2012a
			R: GCCAATGGCAATTACTCGAA		0,2	
	L2	*mHp_077098*	F: TTGATGCGTGATGGTCTTGT	ATTO 550	0,1	
			R: GTAATCCGTCCGGCGTAAA		0,1	
	L3	*mHp_111990*	F: GCCAACAGAACTAACGTGAT	HEX	0,15	
			R: CATGTTACCCCTGTCTTCAT		0,15	
	L4	*mHp_103438*	F: ACTGCTTCTGAACGCTATTC	ATTO 565	0,15	
			R: GGTAGAAACACGAAGGAATG		0,15	
B	L5	*mHp_060142*	F: TGGCTCTCGAGAAAGAGGAG	FAM	0,15	
			R: TTACTCGATTGATCGTCCTT		0,15	
	L6	*mHp_080495*	F: TCAAGACGAGTTGGGTCACA	ATTO 550	0,3	
			R: GCTTGGCGTTATGGTGAGTT		0,3	
	L7	*mHp_080497*	F: CTTGTTGGACTTGCAAGAGT	FAM	0,3	
			R: GTTGGTAGTGGTGGAGGTAA		0,3	
	L8	*mHp_088853*	F: CTGGTCTGGTGTTTTTGATT	ATTO 565	0,25	
			R: CTCCAAAATTCAAGTTCCAC		0,25	
	L9	*mHp_092622*	F: GTCGGCGCTAGTAGAAGCAT	ATTO 565	0,1	
			R: GTGGTTGCACTGAAAGAGAG		0,1	
	L10	*mHp_095478*	F: ATTTTAAACCCCTCGAATAA	HEX	0,6	
			R: ATTTGTGAACCTGCGACTAC		0,6	
C	L11	*mHp_066169*	F: AACGCGTAGAGTAAGTTGGT	ATTO 550	0,2	
			R: ACCTCAAATAGAACGAATGC		0,2	
	L12	*mHp_073013*	F: ACGGCAGAGGAACAATAGCA	ATTO 565	0,25	
			R: TCACGAAGGGAAGAAAGTGG		0,25	
	L13	*mHp_079915*	F: ATCCCACTTCCACCTCCATT	HEX	0,25	
			R: TGAGGAGGACGAGTAGTGTG		0,25	
	L14	*mHp_095481*	F: AGCTTGGTTGTAGCCCAGAG	FAM	0,2	
			R: TATTCCAAGCAGCCGATTCT		0,2	
D	L15	*mHp_068858*	F: ATGTTTTCATGCGGCTCTTC	HEX	0,15	Haňáčková *et al.*, 2015
			R: TTCCGGGAAACAATTACGC		0,15	
	L16	*mHp_076105*	F: CGGGTCTTAATGCTTGGAGAT	ATTO 565	0,15	
			R: CCAGCTATGACAGCGACTTG		0,15	
	L17	*mHp_086811*	F: GACAGGGCGACAATCTCAC	FAM	0,1	
			R: CGGGTGTGGAAGATTGCTA		0,1	
	L18	*mHp_076166*	F: TTCCTTGCCAACTTTATCCTG	ATTO 550	0,1	
			R: TTAGGCACAGCTTTCATAGCC		0,1	

2.5. Microsatellite markers

2.5.1. Multiplex PCR

Each reaction was set up in 10µL volumes containing 1x of S-Buffer (PeqLab), 800µM of dNTPs, 0.5U of Taq polymerase (PeqLab) and 1µL of the template DNA (or PCR water for negative control). 18 microsatellite markers (Gross *et al.*, 2012a; Haňáčková *et al.*, 2015) were amplified in four multiplex PCRs (A, B, C and D). Each one includes 4 to 6 primer pairs in various concentrations (table 3). Every multiplex reaction was completed with PCR water. PCR conditions were 3min at 94°C and continued with 32 cycles at 94°C for 30sec, 56°C for 30sec, 72°C for 90sec then followed by a final extension at 72°C for 5min. PCR amplification was verified on 1.5% agarose gel stained with GelRed Nucleic Acid Gel Stain (Biotum). Gel-electrophoresis was accomplished with 1.7µL of PCR product mixed with 6.2µL of loading buffer. Amplified fragments were visualized on a UV-transilluminator (UVP) after 20min and a 100bp-1kb DNA ladder (Biozym) was included in each gel. This visualization step was only used for determining the dilution for the fragment analysis.

2.5.2. Fragment analysis

Fragment analysis was performed on an ABI 3130xl Genetic Analyser at the Comprehensive Cancer Center DNA Sequencing Facility, University of Chicago (Chicago, USA). Genotypes were scored by analyzing fragment sizes using the software Peak Scanner version 2.0 (Applied Biosystems). Basic statistics were done using GenAlEx (Peakall & Smouse, 2006, 2012).

2.6. Data analysis

For analysis purposes, we assumed that record of the same genotype in sample pairs (petiole and shoot) resulted from the growth of the given genotype from petiole to shoot, rather than from a direct infection. Furthermore, we used 18 species-specific microsatellites with high genotypic diversity. They have a high resolution power which allowed proper differentiation of all strains in the studies by Gross *et al.* (2012a) and Haňáčková *et al.* (2015). The quality of these markers has been assessed in these articles by showing their selective neutrality, their absence of linkage among loci and their Mendelian inheritance. This is why we are postulating here that each genotype corresponds to one individual. Thus, they are referred to as distinguished multilocus genotypes (MLGs).

Isolates of *H. fraxineus* from 42 leaf petiole-shoot pairs were used for the microsatellite analyses. A pair was excluded because of genotyping delays and, for the remaining 11 petiole-shoot pairs, isolation from the petiole failed in four cases and from the shoot in seven cases, and these pairs could thus not be included in the investigations. However, from one shoot (tree n°59) three isolates obtained from three different positions were investigated as well, despite isolation of *H. fraxineus* from the corresponding petiole was unsuccessful. Similarly, from tree n°52 three shoot isolates, also obtained from different positions, were examined, in addition to the petiole isolate. For 39 of the remaining 42 pairs, only one petiole and one shoot isolate (out of up to six which had grown from the different petiole fragments and shoot discs) were chosen for the main data set of the study. Additionally, all six available isolates from three saplings (n°29, n°54 and n°56) from both the petiole and the shoot (36 samples) were investigated. They were chosen because they were among 6 pairs where petiole and shoot isolates had opposite mating type results. The other 3 of such pairs are not included in the presentation of this work because fewer than six isolates per petiole and/or shoot were available. In total, 135 *H. fraxineus* isolates were genotyped.

Table 4: Identification of differentially encoded alleles of polymorphic microsatellite loci of _Hymenoscyphus fraxineus_. Each locus is given a short code name corresponding to their order in table 3. L2 was excluded from further analyses due to its lack of polymorphism. Motif size corresponds to the number of nucleotides repeated, according to Gross _et al._, 2012a and Haňáčková _et al._, 2015.

Locus	Motif size	Number of alleles	Allele size range (bp)
L1	3	3	247-253
L2	3	1	170
L3	3	2	230-236
L4	3	2	213-216
L5	3	2	164-170
L6	2	2	148-154
L7	3	2	245-254
L8	3	2	280-300
L9	3	2	111-117
L10	2	2	233-250
L11	4	2	248-262
L12	2	2	185-240
L13	3	2	184-201
L14	4	3	137-146
L15	3	2	120-129
L16	4	2	197-201
L17	3	2	151-160
L18	3	3	155-187
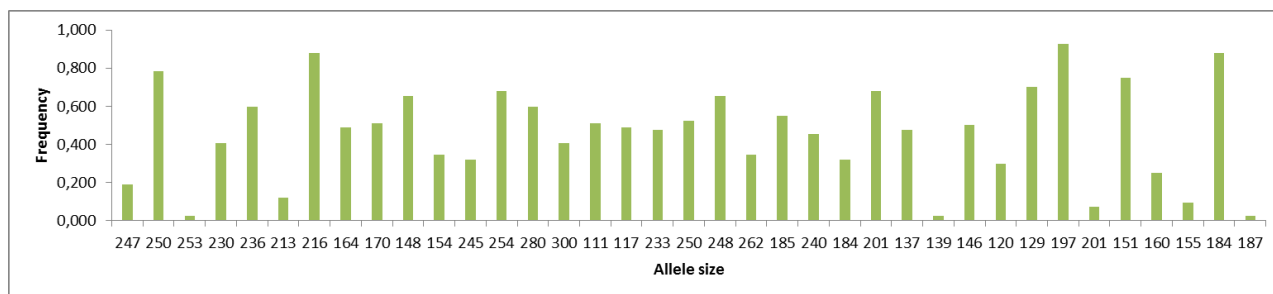
Figure 5: Allelic frequencies of 17 polymorphic microsatellite loci of _Hymenoscyphus fraxineus_.
Allele size corresponds to all identified alleles per locus, summarized in table 4.

3. Results

3.1. Isolation of *H. fraxineus* and other fungi

H. fraxineus was isolated from 50 out of the 54 (92.6%) investigated symptomatic leaf petioles of *F. excelsior*, 36 times (66.7%) in pure culture and 14 times (26%) together with other fungi. Other fungi, various, unidentified species, were obtained from one third of the petioles (18), but only from four petioles they were isolated alone, without *H. fraxineus*. Likewise, the pathogen was recovered from 47 out of the 54 (87.0%) examined shoots with necrotic lesions in the phloem, in 44 cases (81.5%) as the sole fungus and in three cases (5.6%) in mixture with other fungi. In total, other fungi were isolated from six shoots (11.1%), but only from three shoots (5.6%) without *H. fraxineus*. Four shoots (7.4%) did not yield any fungal growth.

3.2. Differentially encoded alleles

Among the 18 microsatellite markers used in the genotyping of *H. fraxineus* strains, we identified 38 different alleles in our population. One microsatellite locus (L2) did not show any polymorphism and thus did not contribute to the overall allelic variability of the investigated fungal population, slightly decreasing the initial discriminatory power of this set of microsatellites markers (table 4).

Generally, we observed low allelic polymorphism. Indeed, 14 microsatellite loci showed a bi-allelic polymorphism and only three were tri-allelic. Moreover, the mean number of effective alleles was around 1.745±0.070. However, the mean Shannon's information index was 0.604±0.033, indicating that even with a low polymorphism the markers were still quite diverse.

More precisely, nine alleles had a frequency below 0.3 and six allelic frequencies were above 0.7 (figure 5). As locus L2 was not taken into account, due to its monomorphic nature, we had 22 out 37 alleles (59%) at mean frequencies of 0.5±0.2, which shows that there is a good allelic repartition in the population and that this microsatellite marker set has still a suitable discriminatory power.

3.3. Genetic profiles

We decided to take into account all genotyped isolates (135 samples), even if some were not used in further analyses (figure 6 and 7), in order to determinate the overall genotypic richness of our *H. fraxineus* population.

Out of the total data set from 135 isolates, 81 different genotypes were detected and assigned to *H. fraxineus* MLGs. If we just take the main data set into account, consisting of 84 isolates (42 petiole-shoot isolate pairs from 42 trees; see figure 6), 63 MLGs were identified. Considering the second data set, obtained from six isolates each from a petiole and corresponding shoot of three seedlings (36 isolates in total), only nine MLGs were detected. As expected, there was less genotypic richness in this set, as in all cases more than one isolate, and often many, from the same petiole-shoot pair belonged to the same genotype.
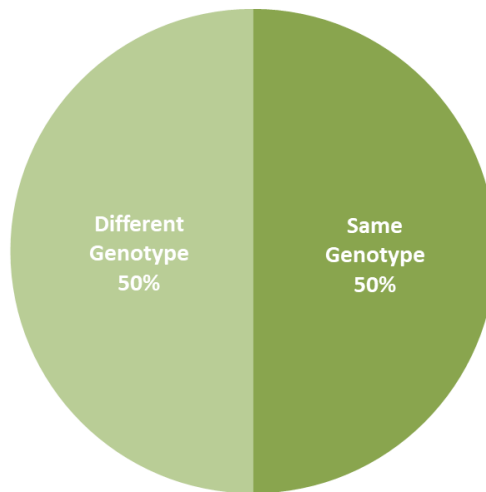
Figure 6: Conformity of distinguished multilocus genotypes (MLGs) of *H. fraxineus* between petiole and shoot samples. It was calculated with frequencies of cases where the MLG of a petiole isolate was identical ("Same genotype") or different ("Different genotype") to the MLG of the corresponding shoot isolate. In 21 trees the same genotype was detected both in the petiole and the shoot, while in 21 trees the petiole and shoot isolates were different genotypes.
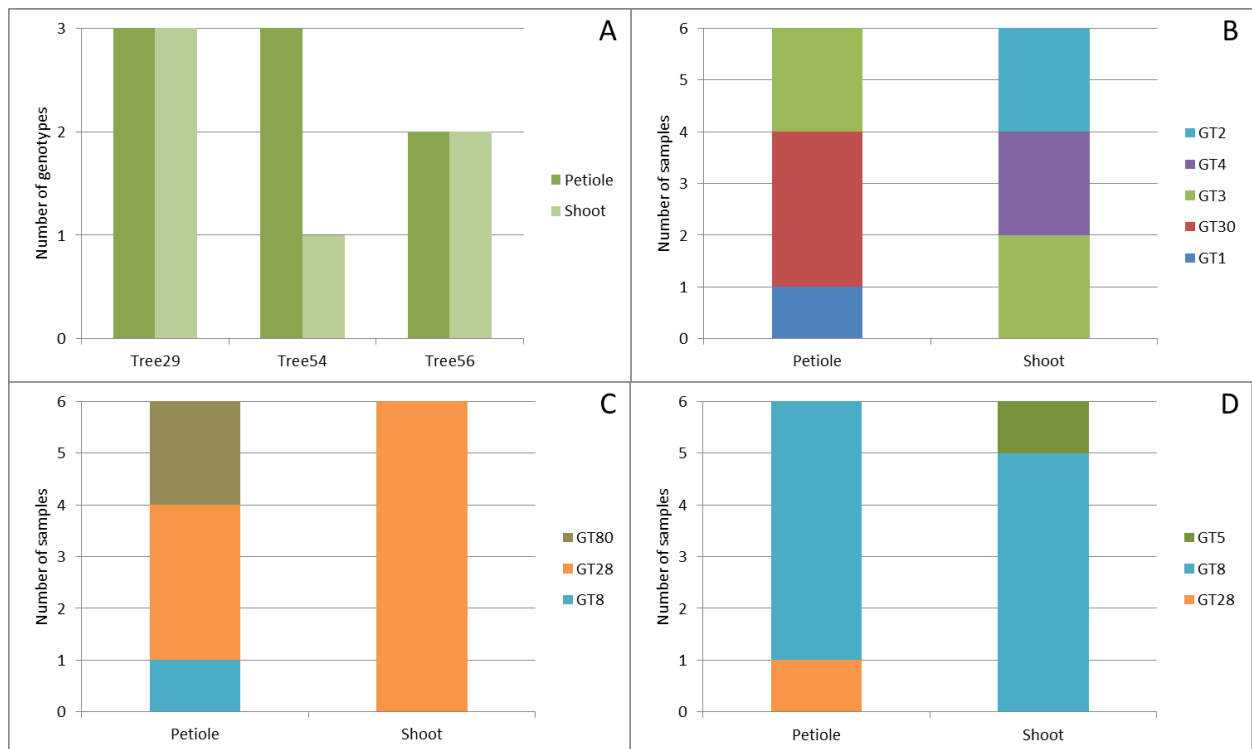
Figure 7: Number of distinct multilocus genotypes (MLGs = GT) of *H. fraxineus* among six isolates each from a petiole and corresponding shoot of each of three different common ash trees. Total number of MLGs present in the petiole and shoot, respectively, of all three trees (A). Number of MLGs present in tree n°29 (B), in tree n°54 (C) and in tree n°56 (D).

3.4. Genotypic continuity

In 21 pairs, the petiole and shoot isolates were confirmed to be genetically identical, whereas in the remaining 21 pairs, they belonged to different genotypes, leading to a perfect 50-50% ratio of cases of genotype continuity or discontinuity in the examined petiole-shoot isolate pairs (figure 6).

3.5. Genotypic diversity

Among the isolate pairs where different genotypes were detected in the petiole and in the corresponding shoot (figure 6), three trees were investigated in more detail, by genotyping further five isolates each from the same petiole and the same shoot (figure 7). The first part of figure 7 (A) shows an overview of the number of genotypes identified among 6 petiole isolates and 6 shoot isolates per tree. It is showing a varying diversity of *H. fraxineus* genotypes in the single petiole and corresponding shoot of the three respective trees, which is even more emphasized in the other three parts of the figure (B-D). In the petiole, three different genotypes were detected in two trees (29 and 54), and two genotypes in one tree (56; figure 7A). In the shoot, the number of different genotypes ranged from one to three (figure 7A).

Tree n°29 had the highest *H. fraxineus* genotypic diversity (figure 7B). Indeed, three MLGs were detected both in the petiole and in the shoot. Initially, GT30 was identified in the petiole and GT3 in the shoot, resulting in a "different genotype" result according to figure 6. Although GT30 was the most frequently isolated genotype (from three fragments) in the petiole, only genotype GT3 was detected both in the petiole and in the shoot, (both two times). In the petiole, a third genotype (GT1), isolated once, was detected, and two further genotypes, GT2 and GT4 (each isolated twice), were detected in the shoot. The two latter genotypes were, however, not confirmed in the petiole.

Tree n°54 had the lowest *H. fraxineus* genotypic diversity in the shoot, as all six isolates were confirmed to belong to a single MLG (GT28; figure 6C). Genotype GT8 was identified in the petiole in the initial analysis, and this pair was thus assigned as "different genotype" pair (figure 6), even though the prevailing genotype in the petiole (3 isolates) was also GT28. Moreover, a third genotype, GT80, was isolated twice.

Finally, tree n°56 showed the highest genotype agreement between petiole and shoot isolates, as MLG GT8 was recovered five times from both the petiole and the shoot (figure 7D). Nevertheless, the isolates used in the initial analysis represented two different genotypes: GT28 in the petiole and GT5 in the shoot. The subsequent did not detect genotype GT28 in the shoot, and GT5 was not recorded on the petiole.

In addition, genotypes GT8 and GT28 were recorded (each one once) in two different trees, n°54 and n°56 (figure 7C; figure 7D).

4. Discussion

4.1. Association of *H. fraxineus* with symptoms of ash dieback

In this work, *H. fraxineus* was isolated at high frequencies from symptomatic organs of *F. excelsior*, from 93.6% of the leaf petioles and 87.0% of the shoots, while other undetermined fungi were obtained much more rarely (from 33.3% of the petioles and 11.1% of the shoots). Moreover, the pathogen was frequently isolated in pure culture, from 66.7% of the petioles and 81.5% of the shoots. These isolation results therefore reinforce, in agreement with previous investigations (e.g. Kowalski 2006; Bakys *et al.*, 2009b; Schumacher *et al.*, 2010; Kowalski *et al.*, 2016; Schwanda & Kirisits 2016), the association of *H. fraxineus* with symptoms of ADB on leaves and woody parts of common ash.

In early studies on ADB, when the cause of the disease was still unknown or debated, *H. fraxineus* was not at all (Przybyl 2002) or at low frequencies isolated from necrotic shoots and twigs of *F. excelsior* (Bakys *et al.*, 2009a). This was likely because in these investigation isolations were made from ash samples showing late stages of disease. In contrast, in the present work, leaves and shoots showing early and fresh symptoms originating from infections in the year of collection were examined, which greatly increases the likelihood to recover the pathogenic but slow growing *H. fraxineus*. Scraping off the epidermis from petioles and the outer bark from shoots had likely also a positive effect on the detection of the pathogen and selected against other fungi, especially endophytic species.

4.2. Confirmation of the leaf petiole-shoot infection path for *H. fraxineus*

Out of the 42 pairs used in the main data set for the microsatellite analyses, 21 presented continuity between petiole and shoot isolates, meaning the same MLG was recorded in both plant organs. Thus, we were able to confirm the colonization path of *H. fraxineus* from leaves to shoots, through the leaf petiole-shoot junction, in 50% of the cases. The number of pairs where different genotypes were detected in the petiole and corresponding shoot was, however, unexpectedly high, as great care was taken to collect plant samples where symptom appearance clearly suggested pathogen progression from the leaf into the shoot (figure 3).

For three trees where different genotypes were initially detected in the petiole and the shoot (with mating type analysis), the subsequent analysis of all six petiole and all six shoot isolates always led to the identification of one genotype occurring in both plant organs (figure 7). This confirmed the progression of the respective genotypes from the petiole to the shoot in these three cases as well. The results of the complete analysis of all isolates from the three trees suggest that more cases of genotypic continuity probably would have been discovered, if more petiole and shoot isolates had been examined for the pairs that gave inconsistent results in the initial microsatellite analysis (figure 6). As *H. fraxineus* is a very slow growing fungus, time was too short to prepare a larger number of isolates from individual petioles and shoots for such more comprehensive analyses.

It is planned to do further analyses in the near future, to strengthen knowledge on the infection biology of the ash dieback pathogen. In fact, the petiole-shoot isolate pair assemblage partly investigated here is a special collection because in most cases infected ash leaves drop prematurely, before necrotic bark lesions become visible (Schwanda & Kirisits, 2016).

Collecting corresponding petiole-shoot isolate pairs for this study was only possible by careful inspection of a large number of seedlings for appropriate symptoms at various dates (T. Kirisits, personal communication). Fixing and careful marking of leaves is an alternative approach, allowing assigning fallen leaves to particular shoot parts (Haňáčková *et al.*, 2017).

In two of the three comprehensively analyzed petiole-shoot isolate pairs, one (tree n° 29) or two (n° 56) additional genotypes, besides the one that was confirmed to have entered from the petiole into the shoot, were detected in the shoot but were not found in the adjacent leaf petiole (figure 7). The origin of these genotypes thus remains unknown. Likely, isolation of these genotypes from the petiole failed or they occurred in the most basal part of the leaf node which was cut away in the course of fungal isolation. They could also represent direct shoot infections or infections from another petiole. The latter is, however, rather unlikely because of the careful inspection of seedlings during sampling. Of course, in pairs where different genotypes were recorded in the petiole and the shoot, alternative infection pathways into the shoot (direct shoot infection, different leaf petiole) may also be possible.

Leaf petioles have been suggested as main infection path of *H. fraxineus* into shoots since the discovery that the fungus' sexual fruiting bodies are formed on leaf petioles and rachises in the leaf litter (Kirisits *et al.*, 2009; Kowalski & Holdenrieder, 2009). Another indication was the frequent appearance of fresh necrotic lesions around leaf scares (figure 3; Kirisits *et al.*, 2009; Bengtsson *et al.*, 2014). Furthermore, *H. fraxineus* proved to be able to infect shoots via artificially inflicted leaf scars (Kräutler *et al.*, 2014). However, the present work is only the second study after the one of Haňáčková *et al.* (2017), where this infection path has been definitely proven.

4.3. Occurrence of identical genotypes on different trees

In the examination of several isolates from the same petiole and shoot of three trees, two MLGs (GT8 and GT28) were found on two different trees (n°54 and n°56), which were growing on the same site (n°10; table 1), relatively close to each other. This finding can have several explanations. First of all, the ascospores responsible for the infections could have had the same parental genotypes, although this is rather unlikely. Another possibility would be that *H. fraxineus* conidia are capable of causing infections, as it has been proposed by Fones *et al.* (2016).

Finally, this result could also question the discriminative power of our set of microsatellite markers to accurately distinguish individuals, as in the study by Haňáčková *et al.* (2017), although we used 6 more microsatellite markers than they did in their study. Also, even though our population showed low allelic polymorphism and no microsatellite locus displayed more than a tri-allelic polymorphism (table 4), this was expected and already taken into account in the design of the combination of markers (Gross *et al.*, 2012a; Haňáčková *et al.*, 2015, 2017).

Moreover, compared to Gross *et al.* (2012a), we had 2 loci (L1 and L14) which were more polymorphic (tri-allelic instead of di-allelic), even though we had one monomorphic locus (L2), showing one less allele than expected. In conclusion, the set of microsatellite markers should have been powerful enough to assign different genotypes accurately.

Besides all suppositions discussed above, I am more inclined to think that the occurrence of the two identical genotypes on two different trees could be due to a mistake. In fact, I have high suspicions that I mismatched the two samples leading to this result during the DNA extraction step, as their codes are very alike (54a-1 and 56a-1). If this were the case and the two isolates can in fact be assigned to the respective other tree, genotype GT8 would be the only one occurring in the petiole of tree n°56, and genotype GT28 would be even more frequent in the petiole of tree n°54 (figure 7).

Furthermore, in the initial analysis of 42 petiole-shoot isolate pairs, we detected 63 MLGs out of the 84 isolates tested. Knowing that in exactly half of our pairs (21) the petiole isolate belongs to the same MLG and that in the other half the petiole and the shoot isolate represent two different MLGs, it means that no identical MLGs occurred on different trees.

$$42\ MLGs + \frac{42\ MLGs}{2} = 63\ MLGs$$

This result tends to invalidate the earlier argument questioning accuracy of the microsatellite markers and supports the view of a possible human mistake. Thus, it would be better to be cautious regarding the occurrence of identical genotypes on different trees (figure 7) and repeat DNA extraction and genotyping for isolates 54a-1 and 56a-1 before drawing any definite conclusions.

4.4. Genotypic diversity in single petioles and single shoots

Up to 3 MLGs were observed within a width of approximately 6 to 12mm (6 consecutive cuts of 1-2mm each), both in petioles and shoots. Furthermore, in some additional sets of isolates, we detected up to 6 MLGs in an approximately 12mm-long section of a petiole (data not shown).

Even if it has previously been described that several genotypes can be found in a single petiole and shoot (Gross *et al.*, 2012a; Bengtsson *et al.*, 2014; Haňáčková *et al.*, 2017), such a small-scale diversity of genotypes as observed here was initially not expected and has not been reported before. Rather, when fungal isolations for this study were made in 2017 and 2018, it was supposed that just a single genotype occurs in the small sampled areas of petioles and shoots.

4.5. Methodological considerations

The fact that only one isolate per plant organ (petiole, shoot) was examined for the majority of isolate pairs (39 out of 42) created an important bias, as in many cases several individuals seem to be able to co-inhabit small areas of tissue. Indeed, the results from just three trees from which not only one but all six isolates per plant organ were analyzed (figure 7) indicate that there may have been a lot of false negative results for the remaining 18 petiole-shoot isolate pairs where different genotypes were recorded (figure 6). Our results (figure 7) demonstrated that analyzing several isolates from each organ (petiole and shoot) is necessary, in order to diminish false negative results in the case of several overlapping MLGs occurring in close physical proximity in petiole and shoot tissues. For the isolate pairs where the genotype in the petiole and the shoot was found to be identical (figure 6), it would be intriguing to know as well whether several genotypes co-inhabit small areas of tissue.

It would also have been desirable to mark the consecutive order of the plant tissue fragments in the course of fungal isolation, as this would have allowed inferring about the spatial distribution of different genotypes along petiole and shoot.

Finally, without substantial statistical analysis, it would be better to stay cautious in interpreting all the results presented here, even if they are largely in agreement with the current understanding of the infection biology and life cycle of *H. fraxineus*. They were supposed to be done but last results of the microsatellite analyses were obtained as late as on the 5th of June only, because of technical difficulties, experimental reworks and delays in genotyping.

In future work, we could use the analysis of molecular variance (AMOVA), considering petiole samples and shoot samples as two sub-populations, in order to see if diversity is significantly different. Such analyses could, for example, clarify whether the passage from the leaf to the shoot via the petiole represents a strong genetic bottleneck for the pathogen as proposed in the study of Haňáčková *et al.* (2015).

5. Conclusions

Using isolation of *H. fraxineus* from symptomatic leaf petioles and adjacent shoots of *F. excelsior* at multiples sites coupled with microsatellite analysis, we were able to confirm the infection route of *H. fraxineus* from a single leaf petiole to the shoot in 50% of the cases. However, it is very likely that a big proportion of our results for the cases where the genotype in the petiole was not identical to that in the shoot represent false negatives. Indeed, we could see in a small sub-set of isolate pairs where genotypes were different in the initial analysis that one genotype occurred in both the petiole and the shoot, when a larger number of isolates per single petiole and shoot was analyzed. These analyses also highlighted the occurrence of several genotypes in small areas of a petiole and shoot. In order to have a more accurate appraisal for the infection path of *H. fraxineus* from a petiole into the adjacent shoot, all pairs should be investigated again using more isolates per plant organ instead of only one.

One of the pitfalls of our study could be the spatial and temporal effects, which we could not evaluate properly. It would have definitely been an improvement of our experiment to include these aspects. If the consecutive order of the fragment cuts for fungal isolation had been marked, it would have been possible to map the location of each genotype in a petiole and shoot on a very fine scale. Also, by doing the same experiment before the appearance of bark necrosis, we could have compared the occurrence and diversity of *H. fraxineus* genotypes in the shoots.

As said earlier, *H. fraxineus* may infect and kill 95% of all common ash trees in Europe. This is why it is very important to enhance our understanding of the disease and the pathogen at all levels, in order to find ways to stop its spread and mitigate its impact. We would then maybe assist to a "Rising out of the ashes" (Muñoz *et al.*, 2016).

6. References

Bakys R, Vasaitis R, Barklund P, Thomsen IM & Stenlid J (2009a) Occurrence and pathogenicity of fungi in necrotic and non-symptomatic shoots of declining common ash (*Fraxinus excelsior*) in Sweden. *European Journal of Forest Research* **128**: 51–60.

Bakys R, Vasaitis R, Barklund P, Ihrmark K & Stenlid J (2009b) Investigations concerning the role of *Chalara fraxinea* in declining *Fraxinus excelsior*. *Plant Pathology* **58**: 284–292.

Bengtsson SBK, Barklund P, von Brömssen C & Stenlid J (2014) Seasonal pattern of lesion development in diseased *Fraxinus excelsior* infected by *Hymenoscyphus pseudoalbidus*. *PLoS ONE* (**9**) e76429: 1–9.

Baral H-O & Bemmann M (2014) *Hymenoscyphus fraxineus* vs. *Hymenoscyphus albidus* – A comparative light microscopic study on the causal agent of European ash dieback and related foliicolous, stroma-forming species. *Mycology* **5**: 228–290.

Baral HO, Queloz V & Hosoya T (2014) *Hymenoscyphus fraxineus*, the correct scientific name for the fungus causing ash dieback in Europe. *IMA Fungus* **5**(1): 79–80.

Chandelier A, Gerarts F, San Martin G, Herman M & Delahaye L (2016) Temporal evolution of collar lesions associated with ash dieback and the occurrence of *Armillaria* in Belgian forests. *Forest Pathology* **46**: 289–297.

Cleary M, Nguyen D, Marčiulynienė D, Berlin A, Vasaitis R & Stenlid J (2016) Friend or foe? Biological and ecological traits of the European ash dieback pathogen Hymenoscyphus fraxineus in its native environment. *Scientific Reports* **6**: 21895.

Cross H, Sønstebø JH, Nagy NE, Timmermann V, Solheim H, Børja I, Kauserud H, Carlsen T, Rzepka B, Wasak K, Vivian-Smith A & Hietala AM (2016) Fungal diversity and seasonal succession in ash leaves infected by the invasive ascomycete *Hymenoscyphus fraxineus*. *New Phytologist* **213**(3): 1405–1417.

Downie JA (2017) Ash dieback epidemic in Europe: How can molecular technologies help? *PLoS Pathogens* **13**(7): e1006381.

Drenkhan R, Solheim H, Bogacheva A, Riit T, Adamson K, Drenkhan T, Maaten T & Hietala AM (2016) *Hymenoscyphus fraxineus* is a leaf pathogen of local *Fraxinus* species in the Russian Far East. *Plant Pathology* **66**: 490–500.

Fones HN, Mardon C & Gurr SJ (2016) A role for the asexual spores in infection of Fraxinus excelsior by the ash-dieback fungus Hymenoscyphus fraxineus. *Scientific Reports* **6**: 34638.

Grad B, Kowalski T & Kraj W (2009) Studies on secondary metabolite produced by Chalara fraxinea and its phototoxic influence on Fraxinus excelsior. *Phytopathologia* **54**: 61–69.

Gross A, Grünig CR, Queloz V & Holdenrieder O (2012a) A molecular toolkit for population genetic investigations of the ash dieback pathogen *Hymenoscyphus pseudoalbidus*. *Forest Pathology* **42**(3): 252–264.

Gross A, Zaffarano, Duo A & Grünig CR (2012b) Reproductive mode and life cycle of the ash dieback pathogen *Hymenoscyphus pseudoalbidus*. *Fungal Genetics and Biology* **49**(12): 977–986.

Gross A, Holdenrieder O, Pautasso M, Queloz V & Sieber TN (2014) *Hymenoscyphus pseudoalbidus*, the causal agent of European ash dieback. *Mol. Plant Pathol.* **15**: 5–21.

Haňáčková Z, Koukol O, Havrdová L & Gross A (2015) Local population structure of *Hymenoscyphus fraxineus* surveyed by an enlarged set of microsatellite markers. *Forest Pathology* **45**: 400–407.

Haňáčková Z, Koukol O, Čmoková A, Zahradník D & Havrdová L (2017) Direct evidence of *Hymenoscyphus fraxineus* infection pathway through the petiole-shoot junction. *Forest Pathology* **47**(6): e12370.

Husson C, Scala B, Cael O, Frey P, Feau N, Ioos R & Marcais B (2011) *Chalara fraxinea* is an invasive pathogen in France. *European Journal of Plant Pathoogy* **130**: 311–324.

Husson C, Caël O, Grandjean JP, Nageleisen LM & Marçais B (2012) Occurrence of *Hymenoscyphus pseudoalbidus* on infected ash logs. *Plant Pathology* **61**: 889–895.

Kirisits T, Matlakova M, Mottinger-Kroupa S, Cech TL & Halmchlager E (2009) The current situation of ash dieback caused by *Chalara fraxinea* in Austria. *Proceedings of the Conference of IUFRO Working Party* 7.02.02 (pp. 97-119), Eğirdir, Turkey, May 2009. SDU Faculty of Forestry Journal, ISSN: 1302-7085; Serial: A, Special Issue.

Kirisits T, Kritsch P, Kräutler K, Matlakova M & Halmschlager E (2012) Ash dieback associated with *Hymenoscyphus pseudoalbidus* in forest nurseries in Austria. *Journal of Agricultural Extension and Rural Development* **4**: 230–235.

Kirisits T, Dämpfle L & Kräutler K (2013) *Hymenoscyphus albidus* is not associated with an anamorphic stage and displays slower growth than *Hymenoscyphus pseudoalbidus* on agar media. *Forest Pathology* **43**: 386–389.

Kirisits T (2017) Further observations on the association of *Hymenoscyphus fraxineus* with *Fraxinus ornus*. *Baltic Forestry* **23**(1): 60–67.

Kjær ED, McKinney LV, Nielsen LR, Hansen LN & Hansen JK (2012) Adaptive potential of ash (*Fraxinus excelsior*) populations against the novel emerging pathogen *Hymenoscyphus pseudoalbidus*. *Evolutionary Applications* **5**: 219–228.

Kowalski T (2006) *Chalara fraxinea* sp nov associated with dieback of ash *(Fraxinus excelsior*) in Poland. *Forest Pathology* **36**(4): 264–270.

Kowalski T & Holdenrieder O (2009) The teleomorph of *Chalara fraxinea*, the causal agent of ash dieback. *Forest Pathology* **39**: 304–308.

Kowalski T, Bilanski P & Holdenrieder O (2015) Virulence of Hymenoscyphus albidus and *H. fraxineus* on Fraxinus excelsior and F. pennsylvanica. *PLoS One* **10**(10): e0141592.

Kowalski T, Kraj W & Bednarz B (2016) Fungi on stems and twigs in initial and advanced stages of dieback of European ash (*Fraxinus excelsior*) in Poland. *European Journal of Forest Research* **135**: 565–579.

Kräutler K, Treitler R & Kirisits T (2015) *Hymenoscyphus fraxineus* can directly infect intact current-year shoots of *Fraxinus excelsior* and artificially exposed leaf scars. *Forest Pathology* **45**: 274–280.

Langer G, Harriehausen U & Bressem U (2015) Eschentriebsterben und Folgeerscheinungen. *AFZ/Der Wald* **70**(20): 22–28.

Marçais B, Husson C, Caël O, Dowklw A, Saintonge F-X, Delahaye L, Collet C & Chandelier A (2017) Estimation of Ash Mortality Induced by *Hymenoscyphus fraxineus* in France and Belgium. *Baltic Forestry* **23**(1): 159–167.

Muñoz F, Marçais B, Dufour J & Dowkiw A (2016) Rising Out of the Ashes: Additive Genetic Variation for Crown and Collar Resistance to *Hymenoscyphus fraxineus* in *Fraxinus excelsior*. *Phytopathology* **106**(12): 1535–1543.

McMullan M, Rafiqi M, Kaithakottil G, Clavijo BJ, Bilham L, Orton E, Percival-Alwyn L, Ward BJ, Edwards A, Saunders DGO, Garcia Accinelli G, Wright J, Verweij W, Koutsovoulos G, Yoshida K, Hosoya T, Williamson L, Jennings P, Ioos R, Husson C, Hietala AM, Vivian-Smith A, Solheim H, MaClean D, Fosker C, Hall N, Brown JKM, Swarbreck, Blaxter M, Downie JA & Clark MD (2018) The ash dieback invasion of Europe was founded by two genetically divergent individuals. *Nature Ecology & Evolution* **2**: 1000–1008.

McKinney LV, Thomsen IM, Kjær ED, Bengtsson SBK & Nielsen LR (2012) Rapid invasion by an aggressive pathogenic fungus (*Hymenoscyphus pseudoalbidus*) replaces a native decomposer (*Hymenoscyphus albidus*): a case of local cryptic extinction? *Fungal Ecology* **5**(6): 663–669.

Mitchell RJ, Beaton JK, Bellamy, Broome A, Chetcuti J, Eaton S, Ellis CJ, Gimona A, Harmer R, Hester AJ, Hewison RL, Hodgetts NG, Iason GR, Kerr G, Littlewood NA, Newey S, Potts JM, Pozsgai G, Ray D, Sim DA, Stockan JA, Taylor AFS & Woodward S (2014) Ash dieback in the UK: A review of the ecological and conservation implications and potential management options. *Biological Conservation* **175**: 95–109.

Peakall R & Smouse PE (2006) GENALEX 6: genetic analysis in Excel. Population genetic software for teaching and research. *Molecular Ecology Notes* **6**: 288–295.

Peakall R & Smouse PE (2012) GenAlEx 6.5: genetic analysis in Excel. Population genetic software for teaching and research-an update. *Bioinformatics* **28**: 2537–2539.

Przybył K (2002) Fungi associated with necrotic apical parts of *Fraxinus excelsior* shoots. *Forest Pathology* **32**: 387–392.

Queloz V, Grünig CR, Berndt R, Kowalski T, Sieber TN & Holdenrieder O (2011) Cryptic speciation in *Hymenoscyphus albidus*. *Forest Pathology* **41**: 133–142.

Schumacher J, Kehr R & Leonhard S (2010) Mycological and histological investigations of *Fraxinus excelsior* nursery saplings naturally infected by *Chalara fraxinea*. *Forest Pathology* **40**: 419–429.

Schwanda K & Kirisits T (2016) Pathogenicity of *Hymenoscyphus fraxineus* towards leaves of three European ash species: *Fraxinus excelsior*, *F. angustifolia* and *F. ornus*. *Plant Pathology* **65**: 1071–1083.

Skovsgaard JP, Thomsen IM, Skovgaard IM & Martinussen T (2010) Associations among symptoms of dieback in even-aged stands of ash (*Fraxinus excelsior* L.). *Forest Pathology* **40**: 7–18.

Sollars ES, Harper AL, Kelly LJ, Sambles CM, Ramirez-Gonzalez RH, Swarbreck D, Kaithakottil G, Cooper ED, Uauy C, Havlickova L, Worswick G, Studholme DJ, Zohren J, Salmon DL, Clavijo BJ, Li Y, He Z, Fellgett A, McKinney LV, Nielsen LR, Douglas GC, Kjær ED, Downie JA, Boshier D, Lee S, Clark J, Grant M, Bancroft I, Caccamo M & Buggs RJ (2017) Genome sequence and genetic diversity of European ash trees. *Nature* **541**(7636): 212–216.

Timmermann V, Børja I, Hietala AM, Kirisits T & Solheim H (2011) Ash dieback: pathogen spread and diurnal patterns of ascospore dispersal, with special emphasis on Norway. *EPPO Bulletin* **40:** 14–20.

Timmermann V, Nagy NE, Hietala AM, Børja I & Solheim H (2017) Progression of Ash Dieback in Norway Related to TreeAge, Disease History and Regional Aspects. *Baltic Forestry* **23**(1): 150–158.

Wey T, Schlegel M, Stroheker S & Gross A (2016) MAT-gene structure and mating behavior of *Hymenoscyphus fraxineus* and *Hymenoscyphus albidus*. *Fungal Genetics and Biology* **87**: 54–63.

Zhao Y-J, Hosoya T, Baral H-O, Hosaka K & Kakishima M (2012) *Hymenoscyphus pseudoalbidus*, the correct name for *Lambertella albida* reported from Japan. *Mycotaxon* **122**: 25–41.

Annexes

Annex I: General information on and results of the mating type determination for all *H. fraxineus* isolates examined in the initial microsatellite analysis.

Annex II: List of all distinguished *H. fraxineus* multilocus genotypes according to their allele size per locus.

Annex I.I: General information and results of the mating type determination for all *H. fraxineus* isolates examined in the initial microsatellite analysis. Differences in the mating type between isolates of the same petiole-shoot pair are marked with red font.

Isolate code	Lab code	Date of sampling	Date of isolation	Site no.	Date of transfer to AMEA	Date of DNA extraction	Mating type
NWE/1/BS	1a	28.08.2016	30.08.2016	1	13.12.2017	12.02.2018	MAT1-2
NWE/1/TR	1b	28.08.2016	30.08.2016	1	13.12.2017	25.01.2018	MAT1-2
NWE/2/BS	2a	28.08.2016	30.08.2016	1	13.12.2017	23.01.2018	MAT1-1
NWE/2/TR	2b	28.08.2016	30.08.2016	1	13.12.2017	25.01.2018	MAT1-1
NWE/3/BS	3a	28.08.2016	30.08.2016	1	13.12.2017	12.02.2018	MAT1-1
NWE/3/TR	3b	28.08.2016	30.08.2016	1	13.12.2017	25.01.2018	MAT1-1
NWE/4/BS	4a	28.08.2016	30.08.2016	1	13.12.2017	23.01.2018	MAT1-1
NWE/4/TR	4b	28.08.2016	30.08.2016	1	13.12.2017	12.02.2018	MAT1-1
NWE/9/BS	9a	30.08.2016	31.08.2016	2	13.12.2017	25.01.2018	MAT1-1
NWE/9/TR	9b	30.08.2016	31.08.2016	2	13.12.2017	29.01.2018	MAT1-1
NWE/10/BS	10a	30.08.2016	31.08.2016	2	13.12.2017	25.01.2018	MAT1-1
NWE/10/TR	10b	30.08.2016	31.08.2016	2	13.12.2017	25.01.2018	MAT1-1
NWE/11/BS	11a	30.08.2016	31.08.2016	2	13.12.2017	29.01.2018	MAT1-1
NWE/11/TR	11b	30.08.2016	31.08.2016	2	13.12.2017	25.01.2018	MAT1-1
NWE/12/BS	12a	30.08.2016	31.08.2016	3	13.12.2017	25.01.2018	MAT1-1
NWE/12/TR	12b	30.08.2016	31.08.2016	3	13.12.2017	25.01.2018	MAT1-1
NWE/13/BS	13a	30.08.2016	31.08.2016	4	13.12.2017	25.01.2018	MAT1-1
NWE/13/TR	13b	30.08.2016	31.08.2016	4	13.12.2017	23.01.2018	MAT1-1
NWE/14/BS	14a	30.08.2016	31.08.2016	4	13.12.2017	29.01.2018	MAT1-2
NWE/14/TR	14b	30.08.2016	31.08.2016	4	13.12.2017	23.01.2018	MAT1-2
NWE/15/BS	15a	30.08.2016	31.08.2016	4	13.12.2017	23.01.2018	MAT1-1
NWE/15/TR	15b	30.08.2016	31.08.2016	4	13.12.2017	25.01.2018	MAT1-1
NWE/16/BS	16a	30.08.2016	31.08.2016	4	13.12.2017	29.01.2018	MAT1-2
NWE/16/TR	16b	30.08.2016	31.08.2016	4	13.12.2017	23.01.2018	MAT1-2
NWE/17/BS	17a	30.08.2016	31.08.2016	4	13.12.2017	25.01.2018	MAT1-1
NWE/17/TR	17b	30.08.2016	31.08.2016	4	13.12.2017	23.01.2018	MAT1-1
NWE/18/BS	18a	30.08.2016	31.08.2016	4	13.12.2017	23.01.2018	MAT1-2
NWE/18/TR	18b	30.08.2016	31.08.2016	4	13.12.2017	23.01.2018	MAT1-2
NWE/19/BS	19a	30.08.2016	31.08.2016	4	13.12.2017	29.01.2018	MAT1-2
NWE/19/TR	19b	30.08.2016	31.08.2016	4	13.12.2017	23.01.2018	MAT1-2
NWE/22/BS	22a	04.09.2016	05.09.2016	4	13.12.2017	25.01.2018	MAT1-2
NWE/22/TR	22b	04.09.2016	05.09.2016	4	13.12.2017	29.01.2018	MAT1-2
NWE/23/BS	23a	04.09.2016	05.09.2016	4	13.12.2017	23.01.2018	MAT1-2
NWE/23/TR	23b	04.09.2016	05.09.2016	4	13.12.2017	25.01.2018	MAT1-2
NWE/24/BS	24a	04.09.2016	05.09.2016	4	13.12.2017	23.01.2018	MAT1-2
NWE/24/TR	24b	04.09.2016	05.09.2016	4	13.12.2017	23.01.2018	MAT1-1
NWE/25/BS	25a	04.09.2016	05.09.2016	4	13.12.2017	25.01.2018	MAT1-2
NWE/25/TR	25b	04.09.2016	05.09.2016	4	13.12.2017	23.01.2018	MAT1-2

Annex I.II: Annex I (continued).

Isolate code	Lab code	Date of sampling	Date of isolation	Site no.	Date of transfer to AMEA	Date of DNA extraction	Mating type
NWE/28/BS	28a	10.09.2016	12.09.2016	7	13.12.2017	23.01.2018	MAT1-1
NWE/28/TR	28b	10.09.2016	12.09.2016	7	13.12.2017	23.01.2018	MAT1-1
NWE/29/BS	29a	10.09.2016	12.09.2016	7	13.12.2017	29.01.2018	MAT1-1
NWE/29/TR	29b	10.09.2016	12.09.2016	7	13.12.2017	12.02.2018	MAT1-2
NWE/30/BS	30a	10.09.2016	12.09.2016	7	13.12.2017	29.01.2018	MAT1-1
NWE/30/TR	30b	10.09.2016	12.09.2016	7	13.12.2017	12.02.2018	MAT1-1
NWE/31/BS	31a	10.09.2016	12.09.2016	2	13.12.2017	25.01.2018	MAT1-2
NWE/31/TR	31b	10.09.2016	12.09.2016	2	13.12.2017	25.01.2018	MAT1-2
NWE/32/BS	32a	10.09.2016	12.09.2016	6	13.12.2017	25.01.2018	MAT1-1
NWE/32/TR	32b	10.09.2016	12.09.2016	6	13.12.2017	12.02.2018	MAT1-2
NWE/34/BS	34a	10.09.2016	12.09.2016	6	13.12.2017	12.02.2018	MAT1-2
NWE/34/TR	34b	10.09.2016	12.09.2016	6	13.12.2017	29.01.2018	MAT1-2
NWE/36/BS	36a	10.09.2016	12.09.2016	4	13.12.2017	29.01.2018	MAT1-2
NWE/36/TR	36b	10.09.2016	12.09.2016	4	13.12.2017	29.01.2018	MAT1-2
NWE/37/BS	37a	10.09.2016	13.09.2016	2	13.12.2017	15.01.2018	MAT1-2
NWE/37/TR	37b	10.09.2016	13.09.2016	2	13.12.2017	25.01.2018	MAT1-2
NWE/39/BS	39a	17.09.2016	19.09.2016	8	13.12.2017	12.02.2018	MAT1-2
NWE/39/TR	39b	17.09.2016	19.09.2016	8	13.12.2017	15.01.2018	MAT1-2
NWE/40/BS	40a	17.09.2016	19.09.2016	8	13.12.2017	12.02.2018	MAT1-1
NWE/40/TR	40b	17.09.2016	19.09.2016	8	13.12.2017	15.01.2018	MAT1-1
NWE/41/BS	41a	17.09.2016	19.09.2016	8	13.12.2017	14.01.2018	MAT1-1
NWE/41/TR	41b	17.09.2016	19.09.2016	8	13.12.2017	15.01.2018	MAT1-1
NWE/42/BS	42a	17.09.2016	19.09.2016	8	13.12.2017	29.01.2018	MAT1-2
NWE/42/TR	42b	17.09.2016	19.09.2016	8	13.12.2017	15.01.2018	MAT1-2
NWE/43/BS	43a	17.09.2016	19.09.2016	7	13.12.2017	14.01.2018	MAT1-1
NWE/43/TR	43b	17.09.2016	19.09.2016	7	13.12.2017	14.01.2018	MAT1-1
NWE/45/BS	45a	17.09.2016	19.09.2016	2	13.12.2017	14.01.2018	MAT1-2
NWE/45/TR	45b	17.09.2016	19.09.2016	2	13.12.2017	14.01.2018	MAT1-2
NWE/46/BS	46a	17.09.2016	19.09.2016	2	13.12.2017	14.01.2018	MAT1-2
NWE/46/TR	46b	17.09.2016	19.09.2016	2	13.12.2017	15.01.2018	MAT1-2
NWE/47/BS	47a	26.10.2016	27.10.2016	2	13.12.2017	14.01.2018	MAT1-1
NWE/47/TR	47b	26.10.2016	27.10.2016	2	13.12.2017	14.01.2018	MAT1-1
NWE/51/BS	51a	26.10.2016	27.10.2016	7	13.12.2017	25.01.2018	MAT1-2
NWE/51/TR	51b	26.10.2016	27.10.2016	7	13.12.2017	15.01.2018	MAT1-2
NWE/52/BS	52a	18.10.2017	20.10.2017	11	12.12.2017	29.01.2018	MAT1-2
NWE/52/TR	52b	19.10.2017	20.10.2017	11	12.12.2017	12.02.2018	MAT1-2
NWE/53/BS	53a	20.10.2017	20.10.2017	6	12.12.2017	12.02.2018	MAT1-2
NWE/53/TR	53b	21.10.2017	20.10.2017	6	12.12.2017	12.02.2018	MAT1-2
NWE/54/BS	54a	22.10.2017	20.10.2017	10	12.12.2017	15.01.2018	MAT1-2
NWE/54/TR	54b	23.10.2017	20.10.2017	10	12.12.2017	29.01.2018	MAT1-1

Annex I.III: Annex I (completed).

Isolate code	Lab code	Date of sampling	Date of isolation	Site no.	Date of transfer to AMEA	Date of DNA extraction	Mating type
NWE/56/BS	56a	24.10.2017	20.10.2017	10	12.12.2017	15.01.2018	MAT1-1
NWE/56/TR	56b	25.10.2017	20.10.2017	10	12.12.2017	15.01.2018	MAT1-2
NWE/57/BS	57a	01.10.2017	20.10.2017	9	12.12.2017	12.02.2018	MAT1-2
NWE/57/TR	57b	01.10.2017	20.10.2017	9	12.12.2017	15.01.2018	MAT1-2
NWE/58/BS-1	58a1	26.10.2017	13.11.2017	9	12.12.2017	15.01.2018	MAT1-2
NWE/58/TR-1	58b1	26.10.2017	13.11.2017	9	12.12.2017	29.01.2018	MAT1-2
NWE/58/TR-2	58b2	26.10.2017	13.11.2017	9	12.12.2017	29.01.2018	MAT1-2
NWE/58/TR-3	58b3	26.10.2017	13.11.2017	9	12.12.2017	29.01.2018	MAT1-2
NWE/59/TR-1	59b1	26.10.2017	13.11.2017	10	12.12.2017	15.01.2018	MAT1-2
NWE/59/TR-2	59b2	26.10.2017	13.11.2017	10	12.12.2017	14.01.2018	MAT1-2
NWE/59/TR-3	59b3	26.10.2017	13.11.2017	10	12.12.2017	29.01.2018	MAT1-2
ZAG/1/BS	Z1a	01.09.2016	01.09.2016	12	13.12.2017	14.01.2018	MAT1-2
ZAG/1/TR	Z1b	01.09.2016	01.09.2016	12	13.12.2017	15.01.2018	MAT1-2

Annex II: List of all distinguished *H. fraxineus* multilocus genotypes according to their allele size per locus. Each locus is given a short code name corresponding to their order in table 3. The color red corresponds to the smallest allele per locus, yellow to the second allele and green to the biggest allele, in the case of a tri-allelic locus.

Genotype	L1	L3	L4	L5	L6	L7	L8	L9	L10	L11	L12	L13	L14	L15	L16	L17	L18
GT1	247	236	216	164	154	245	280	111	233	248	185	184	137	129	197	151	155
GT2	247	236	216	164	154	245	280	111	233	248	185	184	139	129	197	151	155
GT3	247	236	216	164	154	245	280	111	233	248	185	201	137	129	197	151	155
GT4	247	236	216	164	154	245	280	111	233	248	185	201	139	129	197	151	155
GT5	250	236	216	170	154	254	280	117	250	248	185	184	137	120	197	151	155
GT6	247	230	216	164	148	254	300	111	250	248	185	184	137	120	197	160	155
GT7	250	236	213	164	148	254	280	111	250	248	185	184	146	129	197	160	155
GT8	250	236	216	170	154	254	280	117	250	248	185	184	146	120	197	151	155
GT9	250	236	216	170	154	245	280	117	233	248	185	184	137	120	197	160	184
GT10	250	230	216	164	148	245	300	117	233	248	185	184	137	129	197	151	184
GT11	250	230	216	164	148	254	300	111	233	248	185	184	137	129	197	151	184
GT12	250	230	216	164	148	254	280	111	250	248	185	201	137	120	197	151	184
GT13	250	236	216	170	148	254	280	117	250	248	185	184	137	120	197	151	184
GT14	250	236	213	164	148	254	280	111	250	248	185	201	146	129	197	160	155
GT15	247	236	216	170	154	245	280	117	233	262	185	201	146	120	201	160	155
GT16	250	236	216	170	148	245	280	117	250	262	185	201	137	129	197	151	155
GT17	250	236	216	170	148	245	280	117	233	248	185	201	146	120	201	151	184
GT18	250	230	216	164	148	245	280	117	233	248	185	201	146	129	197	160	184
GT19	250	230	216	164	148	254	280	111	250	248	185	201	146	120	197	151	184
GT20	250	230	216	164	148	254	280	111	250	248	185	201	137	129	197	151	184
GT21	250	236	213	164	154	254	280	111	250	248	185	184	146	129	197	151	184
GT22	250	236	213	164	148	254	280	117	233	262	185	184	146	129	197	151	187
GT23	250	230	216	170	148	254	280	111	233	262	185	201	137	129	197	151	184
GT24	247	230	216	164	148	254	300	117	250	248	185	201	146	120	197	160	155
GT25	250	230	216	170	148	254	280	117	250	248	185	184	146	129	197	151	184
GT26	247	236	216	170	154	254	280	111	250	248	185	184	137	129	197	160	184
GT27	250	236	216	170	148	245	280	117	250	262	185	184	139	129	197	151	184
GT28	250	236	216	164	154	254	280	111	233	262	185	201	137	129	197	151	184
GT29	250	230	216	164	148	245	300	117	233	248	185	201	146	129	197	151	184
GT30	247	236	216	170	148	254	300	117	233	248	185	184	146	129	197	151	184
GT31	247	230	216	164	148	245	280	111	233	262	240	184	137	120	197	151	184
GT32	250	230	216	170	148	245	280	111	250	248	185	201	146	129	197	160	184
GT33	247	236	216	164	148	254	300	111	233	248	185	201	146	129	197	151	184
GT34	247	236	216	170	154	254	280	111	250	248	185	184	146	129	197	160	184
GT35	247	236	216	170	154	245	300	111	233	248	185	201	146	129	201	151	184
GT36	250	236	216	170	148	254	280	117	250	262	185	201	137	120	197	151	184
GT37	250	236	216	170	148	245	280	117	250	262	185	201	137	129	197	151	184
GT38	250	236	216	170	154	254	280	111	250	262	185	184	146	129	197	151	184
GT39	250	230	216	170	154	254	300	111	250	248	185	184	146	129	197	151	184
GT40	250	230	216	170	148	245	280	111	250	262	185	201	146	129	197	160	184
GT41	250	236	216	164	148	254	300	117	233	262	185	201	137	129	197	151	184
GT42	250	236	213	170	148	254	300	111	250	248	185	184	146	129	197	160	184
GT43	250	236	216	170	148	254	280	117	250	262	185	201	146	120	197	151	184
GT44	250	230	216	170	154	254	300	111	250	262	185	184	146	129	197	151	184
GT45	250	236	216	170	148	254	280	117	233	248	240	184	137	129	197	151	184
GT46	250	230	216	164	154	254	300	111	250	262	185	201	146	120	197	151	184
GT47	250	236	216	164	148	245	280	111	233	248	240	201	146	129	197	151	184
GT48	247	230	216	164	154	245	280	111	233	262	240	201	137	120	197	160	184
GT49	247	236	216	170	154	245	300	111	233	248	240	184	137	129	201	151	184
GT50	247	230	216	164	148	254	300	117	250	248	240	201	139	120	197	160	155
GT51	250	230	216	164	148	254	300	117	250	248	240	201	137	129	197	151	155
GT52	250	236	216	164	154	245	280	111	233	262	240	201	146	120	197	151	184
GT53	250	230	216	170	148	254	300	117	250	262	185	201	146	129	197	151	184
GT54	250	236	216	164	148	254	280	111	250	262	240	201	137	129	197	160	155
GT55	250	236	216	170	148	254	300	117	233	262	240	184	139	129	197	160	155
GT56	250	230	216	164	148	254	300	117	233	248	240	184	146	129	197	151	184
GT57	250	236	216	170	148	254	280	117	233	248	240	201	137	129	197	151	184
GT58	250	236	216	170	154	254	280	111	250	248	240	184	137	129	197	151	184
GT59	250	230	216	164	154	245	300	117	250	248	240	184	137	129	197	151	184
GT60	250	236	213	164	148	254	280	117	233	262	240	201	137	129	197	151	187
GT61	247	230	216	170	148	254	280	117	250	248	240	201	137	129	197	151	184
GT62	253	230	216	164	148	245	280	117	250	248	240	201	146	129	197	151	184
GT63	250	230	216	164	148	254	300	117	250	262	240	201	137	129	197	151	155
GT64	250	236	216	164	148	245	300	111	250	262	240	201	137	129	197	160	155
GT65	250	236	216	170	148	254	300	111	233	248	240	201	137	129	197	151	184
GT66	253	236	216	164	148	245	280	117	250	248	240	201	146	129	197	151	184
GT67	250	230	216	170	154	254	300	111	250	248	240	184	137	129	197	151	184
GT68	250	230	216	170	148	254	280	111	250	248	240	201	146	129	197	151	184
GT69	250	236	216	170	148	254	300	111	250	262	240	184	137	129	197	160	155
GT70	250	236	216	170	148	245	280	117	250	248	240	201	146	129	197	151	184
GT71	250	230	216	164	154	245	300	117	250	248	240	201	137	129	197	151	184
GT72	250	236	213	164	148	245	300	117	250	262	240	201	137	120	197	151	184
GT73	250	230	216	170	148	254	280	117	250	262	240	201	137	129	197	151	184
GT74	250	236	213	164	148	245	300	117	250	262	240	201	139	120	197	151	184
GT75	250	236	213	164	148	254	300	111	250	248	240	201	146	120	197	160	184
GT76	250	230	216	170	148	254	300	117	250	248	240	201	137	129	197	151	184
GT77	250	236	216	164	148	254	300	117	233	248	240	201	146	129	197	160	184
GT78	250	236	216	170	154	254	300	117	233	248	240	201	139	129	197	160	184
GT79	250	236	216	170	148	245	300	117	250	248	240	201	137	129	197	160	184
GT80	250	236	216	164	148	254	300	117	233	262	240	201	146	129	197	151	184
GT81	250	230	216	170	154	254	300	111	250	248	240	201	146	129	197	151	184

	Diplôme et Mention : Master Biologie, Agrosciences
AGRO CAMPUS OUEST · UNIVERSITÉ DE RENNES 1	Parcours : Amélioration, Production et Valorisation du Végétal
	Option : Physiologie Moléculaire et Adaptations aux Stress
	Responsable d'option : Antoine GRAVOT

Auteur(s) : Astrid KOEHL	Organisme d'accueil : University of Natural Resources and Life Sciences, Vienna (BOKU), Institute of Forest Entomology, Forest Pathology & Forest Protection
Date de naissance : 04/11/1993	
Nb pages : 18 Annexe(s) : 2	Adresse : Peter-Jordan-Straße 82, 1190 Wien, AUSTRIA
Année de soutenance : 2018	Maître de stage : Thomas KIRISITS

Titre français : Confirmation de la propagation de *Hymenoscyphus fraxineus* des feuilles vers les branches de *Fraxinus excelsior*

English title: Confirmation of the colonization path of *Hymenoscyphus fraxineus* from leaves to shoots in *Fraxinus excelsior*.

Résumé :

La chalarose du frêne, causée par *Hymenoscyphus fraxineus*, est une maladie qui a émergé durant les 25 dernières années. Elle fut d'abord observée en Pologne et s'est maintenant étendue à la majorité de l'aire de distribution de son hôte, le frêne commun (*Fraxinus excelsior*). Il a été estimé que *H. fraxineus* pourrait infecter et tuer 95% des frênes commun. Les symptômes de cette maladie incluent un flétrissement du feuillage responsable ensuite d'une descente de cime. Les nécroses corticales sont supposées se développer après une infection venant des pétioles. Le but principal ici a été de confirmer la colonisation de *H. fraxineus* des branches en passant par le pétiole des feuilles de *F. excelsior*. Nous avons utilisé 18 marqueurs microsatellites pour analyser 84 échantillons isolés à partir de fragments de pétioles et de branches de 42 jeunes *F. excelsior*. Les objectifs étaient d'identifier les allèles présents dans notre population, d'établir des profils génétiques pour caractériser les individus, et de confirmer la progression de *H. fraxineus* des pétioles aux branches. Nous avons déterminé que 17 marqueurs étaient polymorphiques et que 14 étaient bi-alléliques. Nous avons distingué 63 différents haplotypes multilocus. La capacité de *H. fraxineus* à infecter les branches à partir du pétiole a été confirmée dans 50% des cas. Nous avons confirmé que la majorité des infections corticales des frênes sont causées par *H. fraxineus* venant des feuilles et passant par la jonction pétiole-branche.

Abstract:

Ash dieback, caused by *Hymenoscyphus fraxineus,* is a disease that has emerged during the past 25 years. It was first observed in Poland and has now expanded over most of the distribution area of its host, the European ash (*Fraxinus excelsior*). It is appraised that *H. fraxineus* may infect and kill 95% of all European ash trees. Ash dieback is associated with numerous symptoms on all plant parts. Necrosis in shoots is assumed to develop after infection through leaf petioles. The main objective of this work was to provide new insights on the life cycle of *H. fraxineus* and, more particularly, on its presumed colonization path from the leaves to the shoots of *F. excelsior.* Here, we used 18 microsatellites markers to analyze 84 isolates obtained from symptomatic petioles and shoots of 42 *F. excelsior* seedlings. The goals of this work were to identify differentially encoded alleles, establish genetic profiles to characterize fungal individuals and confirm the progression of *H. fraxineus* from a petiole into a shoot. We determined that 17 markers were polymorphic and 14 were bi-allelic. Likewise, we distinguished 63 different multilocus haplotypes. Furthermore, the infection route of *H. fraxineus* from a single leaf petiole to a shoot was confirmed in 50% of cases, but the true proportion may be substantially higher. In conclusion, we confirmed here that the majority of ash shoot infections are caused by *H. fraxineus* individuals originating from leaves, entering woody parts through the petiole-shoot junction.

Mots-clés : chalarose du frêne, microsatellite, marqueur génétique, espèce invasive.

Keywords: ash dieback, microsatellite, genetic marker, invasive species.